doi: 10.21495/71-0-343

25th International Conference
ENGINEERING MECHANICS 2019
Svratka, Czech Republic, 13 – 16 May 2019

# NUMERICAL SIMULATION OF SEAL LEAKAGE FLOWS IN AXIAL TURBINE STAGE

**P. Straka*, J. Pelant****

**Abstract:** *The contribution deals with numerical simulation of compressible flow through the axial turbine stage equipped with the hub-seal. The current flowing from the hub-seal has a major impact on the secondary flow in the hub-region of the blade span. The aim of this work is to found a dependency of the efficiency-drop on the hub-seal mass flow rate. Numerical simulation has been made for configuration of experimental axial single-stage reaction turbine.*

**Keywords: Axial turbine stage, secondary flows, hub-seal, efficiency.**

## 1. Introduction

In axial turbine stages the secondary flows have an important impact on the drop of the stage efficiency. Significant sources of the secondary flows are shroud- and hub-seals (Straka, 2018, Straka & Pelant, 2018, Straka et al., 2017). This secondary stream has important impact on the efficiency drop in the axial turbine stages. This paper deals with numerical simulation of the hub-seal leakage flow effect on the axial turbine stage efficiency.

Figure 1a shows the scheme of the simplified axial turbine stage. Simplification lies in the absence of the rotor blade shroud. Next simplification is disconnection of the inlet to the stage and inlet to the hub-seal. The mass flow rate through the hub-seal is controlled with the size of the radial clearance $c_{rad}$ in range from 0.1 mm up to 1.5 mm. The blade span to the mean blade chord ratio is approx. 1.67. Two axial clearances $c_{ax}$ = 5 mm and 10 mm were tested. The inlet boundary to the axial turbine stage lies in distance of 42 mm before the leading edge of the stator blade at the middle diameter, the outlet boundary lies in distance of 42 mm behind the trailing edge of the rotor blade at the middle diameter.

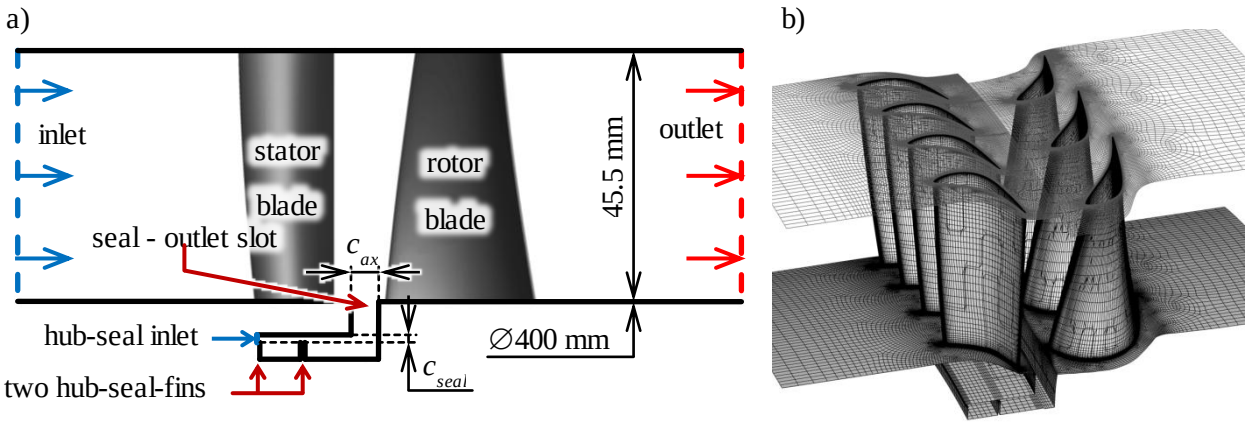


*Fig. 1: a) scheme of the computational domain; b) multi-block structured computational mesh.*

* Ing. Petr Straka, Ph.D.: Czech aerospace research centre; Beranových 130, 199 05 Prague; CZ, straka@vzlu.cz

** RNDr. Jaroslav Pelant, CSc.: Czech aerospace research centre; Beranových 130, 199 05 Prague; CZ, pelant@vzlu.cz

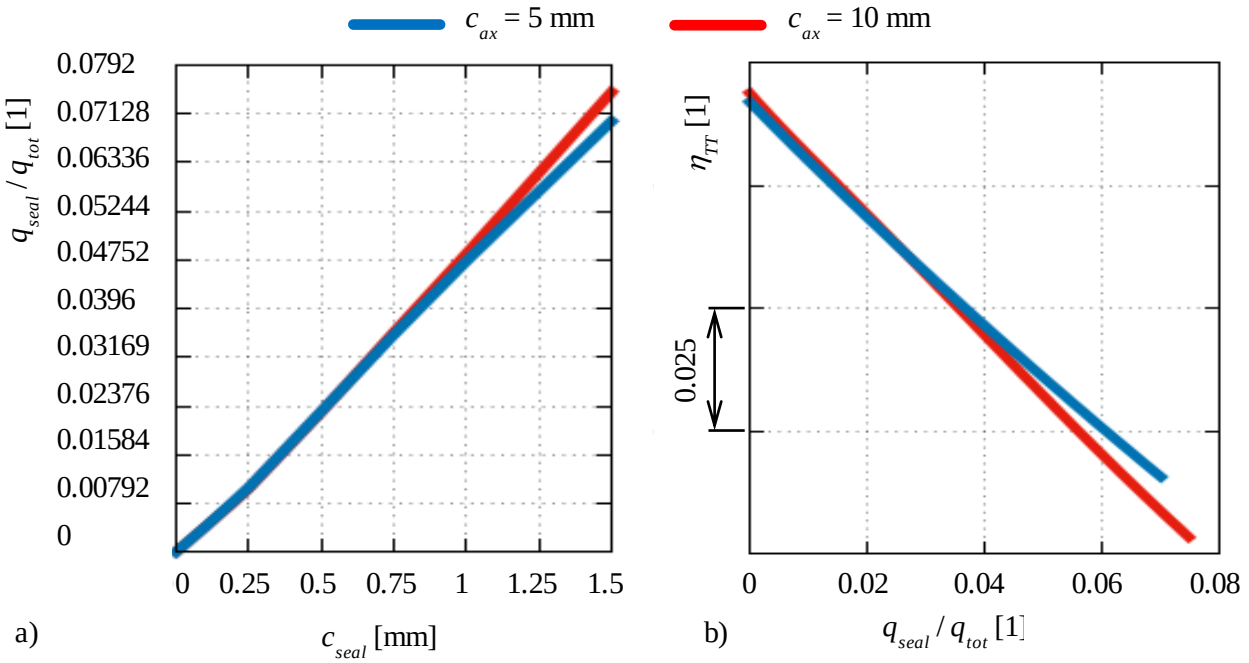


*Fig. 2: a) dependency of the hub-seal mass-flux to total mass-flux ratio on the radial clearance; b) dependency of the total-total efficiency on the hub-seal mass-flux to total mass-flux ratio.*

Two modification of the rotor disc front side at the point of the outlet slot from the hub-seal (see figures 1a and 3) was studied in this work in order to supress negative effect of the secondary flows interaction with the rotor blades.

The isentropic outlet Mach number is $M_{is,out}$ = 0.24, the isentropic outlet Reynolds number is $Re_{is,out} \approx 5.1\times10^6$, rotational speed of the rotor blades is 3810 RPM. The flowing medium is perfect gas of the heats capacity ratio $\gamma$ = 1.2229 and the specific gas constant $R$ = 407.86 J·kg$^{-1}$·K$^{-1}$.

Original count of blades is 78 stator and 56 rotor blades. This count was modified for numerical simulation in order to decrease the computational performance requirements. The computational domain (shown in figure 1b) covers periodically repeated section containing four stator and three rotor blades, where the scale factor of stator blades is $i_s$ = 1.022 and the scale factor of rotor blades is $i_r$ = 0.978. Note that prediction of the secondary flows effect is only slightly affected by scaling of blade geometry when the scale factor is not far from value 1 (as discussed e.g. in Straka & Pelant, 2016 and Straka, 2016).

Calculations of flow were performed using the in-house numerical software, which is based on solution of RANS equations closed with two-equations turbulence model (for more details see Straka, 2012, Straka, 2013 and Straka, 2010). The nonlinear explicit algebraic model of the Reynolds stress is used in this work (Rumsay & Gatski, 2001). Figure 1b shows multi-block structured computational mesh of hexahedral cells with almost $9.1\times10^6$ nodes. The computational mesh is refined close to the walls to ensure that the viscous sub-layer is covered at least by five cells.

At the inlet boundaries (to the axial stage as well as to the hub-seal) there were prescribed the total temperature $T_{T0}$ = 598.107 K, the total pressure $p_{T0}$ = 5.005677 MPa, the inlet turbulence intensity $Tu_0$ = 2.5%, ratio of the turbulent and the molecular viscosity $\mu_t$ / $\mu$ = 100 and axial flow direction. At the outlet boundary there was prescribed the static pressure at the hub diameter $p_{S2}$ = 4.828995 MPa together with the radial equilibrium assumption.

## 2. Numerical results

The solution algorithm was set for unsteady flow – second order accuracy in time and space. Number of the rotational steps $\Delta\varphi$ per periodically repeated section of four stator and three rotor blades was set to $\varphi_{period}$ / $\Delta\varphi$ = 408, it means approx. hundred steps for passing one pitch of the stator blade. After the initial condition disappears the flow field was averaged during three periods. The averaged flow field was then used for evaluation of the mass flux $q_{seal}$ through the inlet boundary to the hub-seal, the total mass flux $q_{tot}$ through the outlet boundary and the total-total efficiency in axial section behind the rotor blades. The

total-total efficiency is defined as $\eta_{TT} = (T_{Tin} - T_T) / (T_{Tin} - T_{Tis})$, where $T_{Tin}$ is the total inlet temperature, $T_T$ is local total temperature and $T_{Tis}$ is local isentropic total temperature.

Dependency of the mass-flux ratio $q_{seal} / q_{tot}$ on size of the radial clearance is shown in figure 2a. We can see that this dependency is nearly linear (which corresponds with Straka, 2018 and Straka & Pelant, 2018) and that the mass flow rate through the hub-seal with radial clearance $c_{seal}$ = 1.5 mm is little bit higher in case of axial clearance $c_{ax}$ = 10 mm. Figure 2b shows dependency of the total-total efficiency $\eta_{TT}$ on the mass-flux ratio $q_{seal} / q_{tot}$. We can see that for higher value of the mass-flux ratio $q_{seal} / q_{tot}$ (radial clearances 1 and 1.5 mm) the case of axial clearance $c_{ax}$ = 10 mm is affected by a larger decrease of the efficiency.

Figure 3 shows basic shape (B) of the rotor disc front side and two modifications (V1) and (V2). Purpose of these modifications is better direction of the secondary vortices going from the hub-seal to the inter-blade channels of the rotor blades (see figure 4b and 4c). Bottom part of figure 3 shows distribution of the total-total efficiency in axial section behind the rotor blades.

Span-wise distribution of the circumferentially averaged total-total efficiency is shown in figure 4a. It is clear that shape of the rotor disc front side has an impact on position and value of maximum efficiency drop in lower part of the rotor blade span. Figures 4b and 4c show isosurfaces of the entropy index $s = p / \rho^{\gamma}$ ($p$ is the static pressure and $\rho$ is the static density) coloured by local turbulence intensity for basic shape (B) and modification (V2).

Averaged values of the total-total efficiency over the entire axial section behind the rotor blades are shown in figure 5. One can see that the (V2) modification brings increasing the efficiency of 0.78 percentage point compared the basic shape (B).

## 3. Conclusions

Presented results demonstrate significant impact of the hub-seal leakage flow on the efficiency drop of the axial turbine stage. We can see that in case of higher mass flow rate through the hub-seal the seal leakage flow is able to knock down the efficiency in lower half of the blade span.

The main aim of this work is demonstrating that it is possible to suppress negative impact of the secondary vortices (going from the hub-seal) by appropriate shaping of the rotor disc front side. Therefore following work will be focused on optimization of the rotor disc front side shape and better direction of secondary flows from the hub-seal.

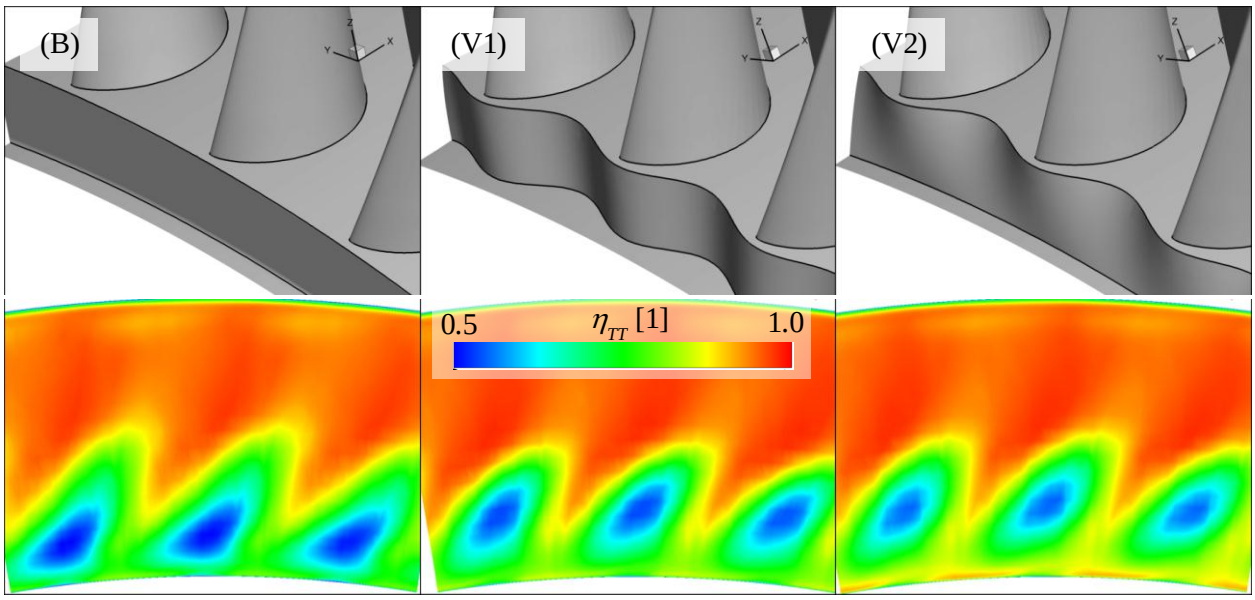


*Fig. 3: Shape of the rotor disc front side (B) – basic, (V1) and (V2) – first and second modification; bottom row: distribution of the total-total efficiency in axial section behind the rotor blades.*

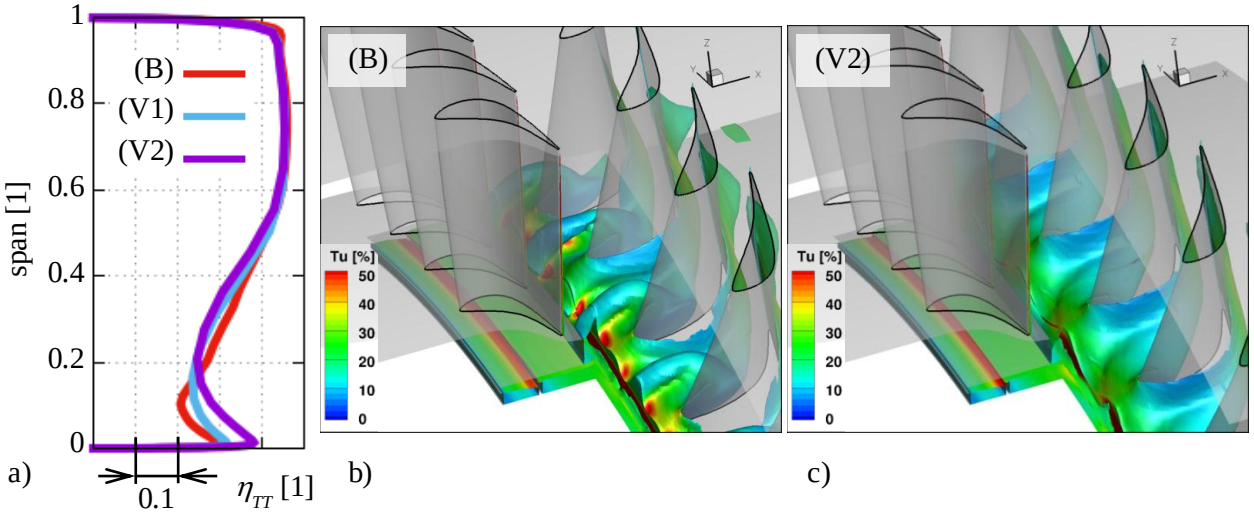


*Fig. 4: a) span-wise distribution of the total-total efficiency; b) and c) isosurface of the entropy index coloured by local turbulence intensity for cases (B) and (V2).*

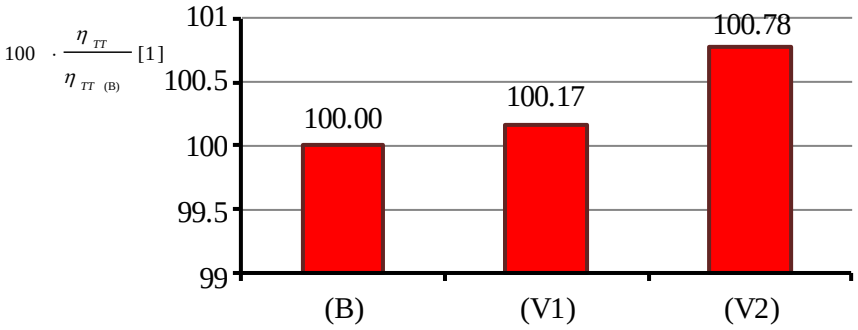


*Fig. 5: Percentage increasing the total-total efficiency compared to the basic shape of the rotor disc front side.*

## 4. Acknowledgement

This work has been supported by the project TH02020086 of the Technology Agency of the Czech Republic.

## References

Straka, P. (2018) Numerical study of shaft-seal parameters for various geometry configuration and operating regimes, *EPJ Web of Conferences* **180**, 02100.

Straka, P. and Pelant, J. (2018) Numerical simulation of flow through a simplified model of the shaft-seal, *Proc. Conf. Engineering Mechanics 2018*, pp 821-824, Svratka.

Straka, P., Pelant, J., Němec, M., Jelínek, T., and Milčák, P. (2017) Investigation of flow in axial stage of experimental turbine, *EPJ Web of Conferences* **143**, 02117.

Straka, P. and Němec, M. (2016) Influence of the radial gap under the stator blade on flow around the hub-end of the rotor blade, *Applied Mechanics and Materials*, **821**, pp. 120-128.

Straka, P. (2016) Modelling of unsteady secondary vortices generated behind the radial gap of the axial turbine blade wheel, *Proc. ECCOMAS Congress 2016*, Crete.

Straka, P. (2012) Simulation of a 3D unsteady flow in an axial turbine stage, *EPJ Web of conferences*, **25**, 01090.

Straka, P. (2013) Calculation of 3D unsteady turbulent flow in low-power experimental axial turbine stage, *Report VZLÚ R-5904*, Prague, (in Czech).

Straka, P. (2010) Calculation of 3D unsteady inviscid flow in turbine stage ST6, *Report VZLÚ R-4910*, Prague, (in Czech).

Rumsay, C.L., Gatski, T.B. (2001) Recent turbulence model advances applied to multi-element airfoil computations, *Jour. Of Aircraft*, **83**, pp. 904-910.